Sains Malaysiana 52(5)(2023): 1435-1451
http://doi.org/10.17576/jsm-2023-5205-09

Effect of Alkali Treatment and Fibre Composition on the Performance of Pineapple Leaf Fibre-Polyvinyl Alcohol Composites

(Kesan Rawatan Alkali dan Komposisi Serat terhadap Prestasi Komposit Alkohol Serat-Polivinil Daun Nanas)

Hanis Nurafiqah Zubairi[1], Noordini M. Salleh[2] & Nor Mas Mira Abd Rahman[1,*]

[1]*Department of Chemistry, Faculty of Science, Universiti Malaya, 50603 Kuala Lumpur, Federal Territory, Malaysia*
[2]*Centre for Fundamental and Frontier Sciences in Nanostructure Self-Assembly, Department of Chemistry, Faculty of Science, Universiti Malaya, 50603 Kuala Lumpur, Federal Territory, Malaysia*

Received: 18 October 2022/Accepted: 7 April 2023

ABSTRACT

This paper studied the properties of composites based on polyvinyl alcohol reinforced with pineapple leaf fibres (PALF/PVA). The surface of pineapple leaf fibres (PALF) has been previously treated with 6% sodium hydroxide solution. The influence of fibre loading and fibre surface treatment were examined. Analysis by Fourier transform infrared spectroscopy (FTIR), and X-ray diffraction (XRD) displayed physico-chemical changes on treated PALF/PVA composites compared to untreated PALF/PVA composites. The results from thermogravimetric analysis (TGA) showed that the introduction of untreated PALF into the composites enhanced the thermal stability of the composites. Progressive improvement of thermal stability was discovered by associating treated PALF with the composites. The treated PALF composites produced also improved mechanical properties with increasing fibre content. Differential scanning calorimetric (DSC) analyses showed no significant changes in melting temperatures upon incorporating untreated PALF into the PALF/PVA composites. The best improvement in tensile strength value was obtained for treated PALF composite having 3 wt% of fibre loading, with enhancements of about 11% and 54%, compared to untreated PALF composites and plain PVA matrix, respectively.

Keywords: Alkali treatment; interfacial adhesion; MD2-pineapple leaf fibres; polymer composites; polyvinyl alcohol

ABSTRAK

Kertas ini mengkaji sifat komposit berdasarkan polivinil alkohol yang diperkuat dengan serat daun nanas (PALF/PVA). Permukaan serat daun nanas (PALF) sebelum ini telah dirawat dengan larutan natrium hidroksida 6%. Pengaruh komposisi serat dan rawatan permukaan serat telah dikaji. Analisis oleh transformasi Fourier inframerah (FTIR) dan pembelauan sinar-X (XRD) memaparkan perubahan fiziko-kimia pada komposit PALF/PVA yang dirawat berbanding komposit PALF/PVA yang tidak dirawat. Keputusan daripada analisis termogravimetri (TGA) menunjukkan bahawa kehadiran PALF yang tidak dirawat ke dalam komposit meningkatkan kestabilan terma komposit. Peningkatan progresif kestabilan terma ditemui dengan kehadiran PALF yang dirawat di dalam komposit. Peningkatan kandungan serat yang dirawat di dalam komposit juga didapati menyebabkan peningkatan dalam sifat mekanikal. Analisis kalorimetrik pengimbasan pembezaan (DSC) menunjukkan tiada perubahan ketara dalam suhu lebur apabila PALF yang tidak dirawat digabungkan ke dalam komposit PALF/PVA. Penambahbaikan paling terbaik dalam nilai kekuatan tegangan diperoleh oleh komposit dengan PALF yang dirawat pada kandungan serat 3 wt% dengan peningkatan sebanyak 11% dan 54%, berbanding komposit PALF yang tidak dirawat dan matriks PVA.

Kata kunci: Komposit polimer; lekatan antara muka; polivinil alkohol; rawatan alkali; serat daun nanas MD-2

Introduction

Widespread consumption of petroleum-based plastics has spurted the ever-expanding environmental pressure. The latest report published by World Wide Fund for Nature (WWF), which scrutinised plastic packaging in Southeast Asia and China issues, reported that Malaysia had been ranked highest in annual per capita plastic packaging consumption (WWF Releases Report Proposing Effective Solution to Mitigate Plastic Pollution in Malaysia 2020). Due to this, the plastic waste always

ends up in landfills and eventually into the rivers and seas, creating an alarming global environmental pollution. The utilisation of natural fibre as reinforcement in the polymer composites is a preferred solution to petroleum depletion problems, degradability and landfill issues. These composites have been taking the central attention in almost every material research community. Natural fibre composites present many advantages besides being biodegradable and renewable. These include excellent specific strength and modulus, low cost, low density, lightweight and safe manufacturing process (Fiore, Di Bella & Valenza 2015).

Malaysia plays a significant role in the world pineapple trade. Malaysia Pineapple Industry Board (MPIB), responsible for the development and production of pineapple in Malaysia, has projected the plans to increase the country's area of pineapple plantations to 20,000 hectares to meet both domestic and international demands. MPIB also reported that the MD2 pineapple cultivar had been chosen to be promoted in industrial planting due to its exceptional qualities. The agro-waste of MD2 pineapple in Malaysia can reach up to 1 304 442 metric tonnes per year. Pineapple leaf fibres (PALF), having known to possess excellent mechanical strength, are not only renewable but are also relatively inexpensive and naturally abundant. By taking the benefits of PALF, more valuable materials can be achieved by substituting glass fibres and any other synthetic fibres currently used to be reinforced with polymers.

Despite the benefits, there are a few difficulties that we need to take into account, such as the incompatibility of natural fibres with some polymer matrices and poor wettability. Currently, polyvinyl alcohol (PVA) has been broadly used with the lignocellulosic fibres to produce natural fibre reinforced polymer composites. The presence of –OH groups in the PVA makes it compatible with the hydrophilic nature of the natural fibres. It is a universal polymer, known to acquire properties such as water solubility, biodegradability, ease to utilise, and film-forming properties (Kalambettu et al. 2015).

Among various chemical treatments, alkali treatment is one of the best surface modification techniques that have been widely used in natural fibre composites. NaOH solution is used to break hydrogen bonds in the cellulosic fibre network structure, enhancing the fibre surface's roughness (Akhtar et al. 2016). In this work, both untreated and alkali treated PALF fibres were used to reinforce PVA matrix to form composite materials. The morphological study, as well as thermal and mechanical properties, were determined at different fibre compositions (1, 2, 3 wt%).

It should be mentioned that there are several cultivars of pineapples, and each has unique qualities both in the physical and mechanical characteristics. Most of the previous researches focused their studies on other popular pineapple cultivars like Josapine, Morris Gajah and Sarawak (Mohamed 2009). However, to the best of our knowledge, no comprehensive work was dedicated to research involving composites reinforced with PALF fibre from MD-2 pineapple cultivar. Therefore, this research aims to utilize PALF from MD-2 cultivar as reinforcement for biodegradable polymer composite and investigate the influence of fibre loading and surface treatment on the properties of PALF/PVA composites in the hope that it will bring benefits to the environment and reduce environmental pollution.

Materials and Methods

Materials

The material used for the PALF/PVA composites is polyvinyl alcohol powder (PVA) (hydrolysis rate: 87.0 - 89.0 mol%) and pineapple leaf fibres (PALF) of MD2 cultivar. The other reactants used included distilled water and sodium hydroxide (NaOH). Both PVA powder and sodium hydroxide pellets were purchased from Chemiz (M) Pte. Ltd.

Extraction of Pineapple Leaf Fibres (PALF)

PALF was extracted using a roller and bladder machine known as PALF M1. The blades of the machine were used to remove the waxy layer of pineapple leaves without damaging the structure of PALF. Next, the PALF was washed with water to eliminate impurities and dried under the sunlight for 1 to 2 days.

Fibre Surface Treatment

From the previous studies, 6% sodium hydroxide (NaOH) concentration is found to be the optimum alkali treatment for PALF to remove all unwanted impurities from the fibre surface (Asim et al. 2018; Zin et al. 2018). PALF was soaked in NaOH solution (6% w/v) in a water bath at room temperature for 6 h. Next, the fibres were washed thoroughly with running water until no alkalinity detected and the pH values were neutralized. After washing, the fibres were then dried in an oven at 80 °C for 48 h to remove the water content.

FABRICATION PROCESS OF COMPOSITES

The treated PALF (TPALF), as well as untreated PALF (UPALF), were cut into 6 mm by using a fibre-cutting machine provided by Malaysia Timber Industry Bio-composite (MTIB) to produce short PALF.

Melt processing technique

Different compositions of PVA and untreated/treated PALF were compounded using the co-rotating twin-screw extruder (LabTech Engineering, Thailand) with a screw diameter of 26 mm. The temperature profile from the hopper to the die was set at 210 °C for five different heating zones under optimum processing conditions. The mixing temperature was set based on the melting temperature of PVA, which was 180 °C. The extruded strand was pelletised into a length of about 6 mm using a pelletiser. Extruded pellets will be dried in the vacuum oven at 95 °C for 24 h prior to the hot compression molding process. Thin films of neat PVA and composites with different fibre compositions were prepared by the hot compression technique. The extruded pellet samples were placed in between two steel mold plates. The plates were pre-heated for 2 min and pressed under a pressure of 40 bar at a temperature of 180 °C for 5 min of contact time. In order to eliminate air bubbles, the samples were repeatedly pressurised and depressurised. The samples were cooled down to room temperature at the pressure of 40 bar for 5 min. The thickness of composite films was controlled at 0.5 mm. The produced films were referred to as shown in Table 1.

CHARACTERIZATION AND TESTING

FTIR Spectroscopy

Fourier-transform infrared (FTIR) spectroscopy analysis was used to characterise the chemical composition of the fibres before and after the surface treatment. The FTIR samples were recorded with a Spotlight 400 Perkin Elmer spectrometer (Waltham, MA, USA) in the absorbance range of 4000 to 400 cm^{-1}. The spectrometer was used together with universal attenuated total reflectance (ATR) accessory for 64 scans at a resolution of 4 cm^{-1}.

Thermogravimetric Analysis (TGA)

Thermogravimetric analysis of PALF/PVA composites was performed using Perkin Elmer TGA 4000 instrument to evaluate the thermal stability of the composite materials at a heating rate of 10 °C min^{-1}. The analysis was operated under a nitrogen atmosphere with a nitrogen flow rate of 20 mL min^{-1} at a temperature range of 25 to 900 °C.

TABLE 1. Formulation of PALF/PVA composite for melt processing technique

Sample	Alkali treatment	Fibre composition (wt%)	Weight of PVA (g)	Weight of PALF (g)
PVA	-	0	1000	0
1UPALF/PVA	Untreated	1	990	10
1TPALF/PVA	Treated			
2UPALF/PVA	Untreated	2	980	20
2TPALF/PVA	Treated			
3UPALF/PVA	Untreated	3	970	30
3TPALF/PVA	Treated			

Differential Scanning Calorimetry (DSC)

Differential scanning calorimetry was carried out with a TA DSC Q20 instrument to identify the phase transitions of the composites. The thermal history of the samples was removed by subjecting the samples to heat scanning from 25 °C to 180 °C, followed by quenching the sample to -30 °C and finally heating again to 200 °C at a heating and cooling rates of 10 and 20 °C min^{-1}, respectively. The analysis were performed under a nitrogen atmosphere at a flow rate of 20 mL min^{-1} to prevent oxidation.

X-ray Diffraction (XRD)

X-ray diffraction (XRD) analysis was operated to investigate the crystallinity of composite materials. XRD patterns of the composites were done through PANalytical Model Empyrean under CuKα radiation (k = 0.1541 nm) at the operating voltage and current of 30 kV and 20 mA, respectively. The samples were scanned over an interval of 2θ = 2°- 30°. XRD patterns were smoothed, and a software-generated parabolic curve corrected the baseline. The composites crystallinity index (CI) was determined based on the ratio of the crystalline region's area to the total area using Equation (1):

$$\mathrm{CI}(\%) = \frac{\text{Area of crystalline peaks}}{\text{Area of all peaks(crystalline+ amorphous)}} \times 100 \quad (1)$$

TENSILE TESTING

Evaluation of the tensile properties of neat PVA, treated and untreated PALF/PVA composites were prepared according to the ASTM D882 (McKeen 2017). The samples were cut into rectangular strips of 70 mm × 10 mm. The test was performed using a Shimadzu AGS-X universal testing machine equipped with a tension load-cell capacity of 5 kN at a constant crosshead speed of 2 mm min^{-1} at room temperature. The initial gap separation was fixed at 30 mm. At least five replicates were carried out for each sample.

Results and Discussion

STRUCTURAL CONFIRMATION

FTIR spectroscopic analysis has been examined on both UPALF and TPALF fibre with the goal of identifying changes in the chemical structure of the fibre brought on by the alkali treatment, that ultimately leads to better adhesion between the components. Figure 1 shows the FTIR spectra of PVA, UPALF, TPALF and 2TPALF/PVA composite. Meanwhile, their main vibrational band frequencies are tabulated in Table 2. In Figure 1(a), all major peaks related to hydroxyl and acetate groups of PVA are shown in the FTIR spectrum. More specifically, the broad peak observed between 3550 and 3200 cm^{-1} is associated with the O—H stretch from the intermolecular and intramolecular hydrogen bonds. The peak observed between 2840 and 3000 cm^{-1} is the result of the C—H stretch from alkyl groups, and the peaks between 1730 and 1680 cm^{-1} are due to the C=O and C—O stretches from the remaining acetate groups in PVA (Asim et al. 2015).

It is known that PALF is made of 80% cellulose and 12% lignin (Asim et al. 2015). FTIR spectra of PALF before and after alkali treatment were shown in Figure 1(b) and 1(c), respectively. For both untreated and treated PALF, the major characteristic peak around 2900 cm^{-1} is related to the symmetric stretching of methyl groups of cellulose. The FTIR spectrum of UPALF displayed in Figure 1(b) indicates the presence of lignin by the appearance of a peak at around 1500 cm^{-1} which corresponds to the vibrations of aromatic rings in lignin. Lignin is a highly complex and aromatic polymer of phenyl propane units, amorphous, and binds to crystalline cellulose with the hemicellulose within the cell wall (Amiandamhen, Meincken & Tyhoda 2020). Though the chemical structure is extremely complex, it is generally accepted that lignin is formed via irregular biosynthesis process constructed from 3 basis phenylpropanoid monomers which are p-hydroxyphenyl (H), guaiacyl (G) and syringyl (S) units (Lu et al. 2017). In addition, a small peak observed in the region of 1729 cm^{-1} was associated with the carboxylic ester (C=O) related to hemicellulose.

After PALF fibres were subjected to alkali treatment, the intensity of the OH peak at 3335 cm^{-1} was found to be slightly increased, as shown in Figure 1(c). According to a previous study, this treatment removed a certain amount of lignin, wax and oils covering the external surface of the fibre cell wall, depolymerizes cellulose and increased the amount of cellulose exposed on the fibre surface (Chand & Fahim 2021). As shown in Equation (2), adding aqueous sodium hydroxide (NaOH) to natural fibre will promote the ionization of the hydroxide group to alkoxide, which acts as a reaction site for fibre-matrix interactions. Alkali treatment dramatically improves the number of reaction sites, consequently increasing

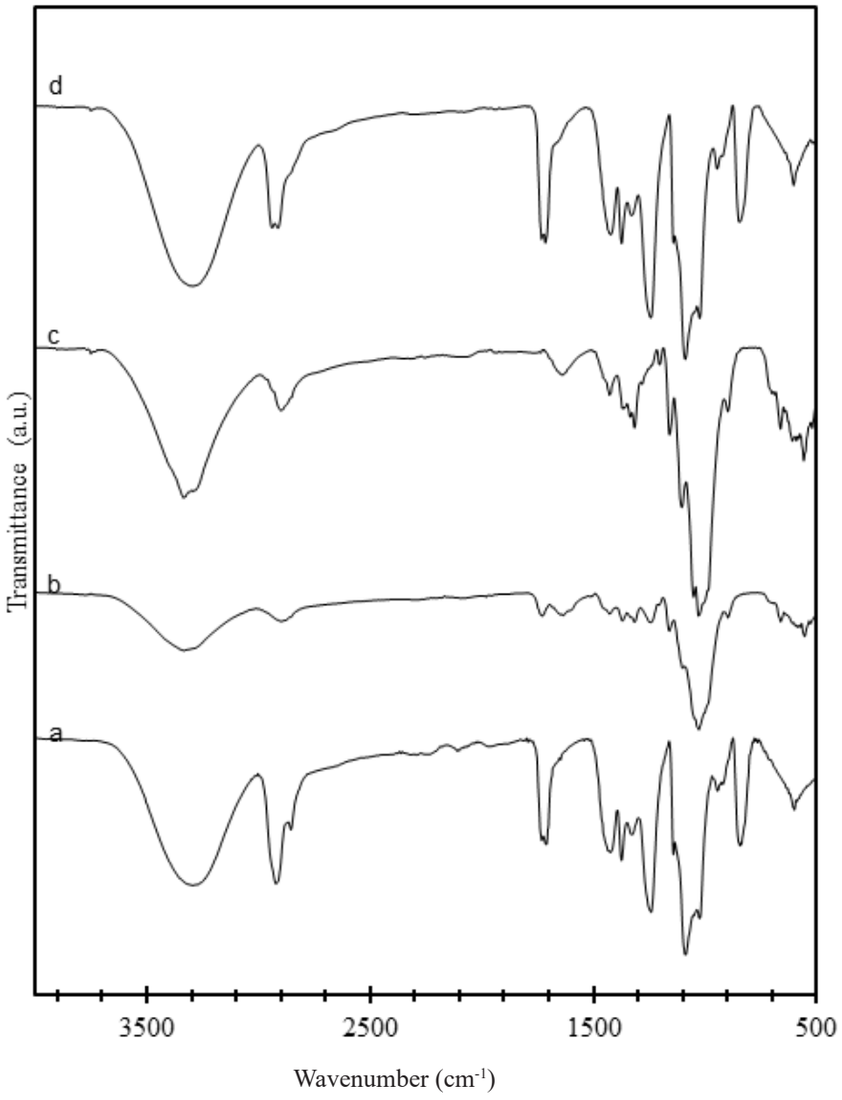

FIGURE 1. FTIR analysis of (a) PVA; (b) UPALF; (c) TPALF; (d) 2TPALF/ PVA composite

the possible interactions between the fibre and polymer matrix, mainly consisting of hydrogen bonding.

Therefore, the peak intensity corresponded to this OH stretching increases. It is also clearly noticeable that the peak around 1729 and 1242 cm^{-1} corresponding to the non-cellulosic components, such as pectin, waxes, and lignin disappeared, suggesting that alkali treatment effectively removed unwanted content from the fibre surfaces. The same observation was discovered in a study done by Akhtar et al. (2016) where the peak disappearance at 1635 cm^{-1} of treated kenaf fibres verified the removal of lignin after the treatment of kenaf fibres. Consequently, better interfacial adhesion between the TPALF and PVA matrix is achieved upon alkali treatment, leading to the improved mechanical properties of the composites which will be discuss further in 'Tensile Properties' section.

$$\text{Fibre} - \text{OH} + \text{NaOH} \rightarrow \text{Fibre} - \text{O}^{-} - \text{Na}^{+} + \text{H}_2\text{O} \qquad (2)$$

TABLE 2. FTIR peak assignments for PVA, PALF, and PALF/PVA composite films

Wavenumber (cm^{-1})	Functional group assignment	References
PVA		
3290	O–H stretching vibration	(Kalambettu et al. 2015; Peresin et al. 2010)
2922	C–H stretching vibration	(Kalambettu et al. 2015; Peresin et al. 2010)
1732	C=O stretching vibration	(Peresin et al. 2010)
1140	C–O stretching vibration	(Jayasekara et al. 2004)
UPALF		
3335	O–H stretching vibration (cellulose)	(Kalambettu et al. 2015)
2901	C–H stretching vibration (cellulose & hemicellulose)	(Kalambettu et al. 2015; Lopattananon et al. 2006)
1729	C=O stretching vibration (hemicellulose & lignin)	(Lopattananon et al. 2006; Nopparut & Amornsakchai 2016; Sarah et al. 2018)
~1590−1610	C=C stretching vibration from aromatic ring (lignin)	(Kalambettu et al. 2015; Sarah et al. 2018)
1242	C−O stretching (hemicellulose & lignin)	(Nopparut & Amornsakchai 2016)
TPALF		
3293	O–H stretching vibration	(Kalambettu et al. 2015)
2PALF/PVA composites		
3290	O–H stretching vibration	(Kalambettu et al. 2015)

Following the incorporation of 2 wt% of TPALF into the PALF/PVA composite system, Figure 1(d) showed most of the composite characteristic peaks is still associated with the matrix PVA. It was determined that the stretching O-H from intramolecular and intermolecular hydrogen bonding was responsible for the broad peak observed at 3290 cm^{-1}. Most remarkably, the peak intensity corresponded to this broad peak was slightly increased as compared to the peak at PVA spectrum. It could be suggested that the amount of OH groups of the fiber increase the overall OH groups in the composite system, indicating an interaction between the PALF and PVA matrix.

THERMOGRAVIMETRIC ANALYSIS (TGA)

Thermogravimetric analysis (TGA) was adopted to examine the thermal stability, decomposition, and mass

change of composites. The TGA thermogram of PVA, PALF, and PALF/PVA composite films with various PALF compositions are illustrated in Figure 2 in the form of percentage weight change versus temperature. Table 3 presents the quantitative values of the vital degradation temperatures, which are the temperature at the intersection point between the initial slope and after the actual decomposition or known as onset temperature (T_{onset}), the derivative peak degradation temperature with maximum weight loss rate (DT_p), and the temperature at 5, 10, and 50% weight loss, which are signified as $T_{5\%}$, $T_{10\%}$, and $T_{50\%}$, respectively.

From the TGA thermogram of neat PVA in Figure 2, a single degradation step was observed where the PVA matrix completely decomposed within a temperature range of 263 °C to 440 °C, with DT_p recorded at 381 °C. The same observation was reported in a study conducted by Peng and Kong (2007) with the peak degradation temperature of PVA at 350 °C. Meanwhile, the neat UPALF degraded in two major step processes. The first step was at a temperature range from 29 °C to 165 °C, with a weight loss of 6.9%. According to the previous study done by Islam, Pickering and Foreman (2011) the weight loss of this stage was due to the vaporization of the absorbed moisture from the fibers. The second step of thermal degradation occurred between 238 °C and 490 °C, with DT_p recorded at 404 °C, which was related to the degradation of cellulosic substances. Almost identical results have been reported in one study by Fan and Naughton (2016) in the case of hemp fibers in the 200-300 °C region, the cellulose in the secondary cell wall begins to decompose, resulting in the formation of volatiles, non-combustible gas, tar, and some char. Cellulose itself has crystalline and amorphous parts. The amorphous region will deteriorate faster than the crystalline region with higher thermal stability.

Further down the line is the decomposition of the lignin. Lignin comprises a highly branched phenolic polymer formed via an irregular biosynthesis process constructed from phenylpropane monomers by the chemical linkages of alkyl-alkyl alkyl-aryl, and aryl-aryl groups (Lu et al. 2017). These carbon-carbon bonds between the structural units give rigidity to plant material. The irregular biosynthesis of lignin caused the lignin content and composition to vary significantly in different fibers (Lu et al. 2017). Hence, lignin cannot be resolved by the general decomposition method. Therefore, it is generally accepted that thermal decomposition of lignin occurred over a wide temperature range beginning at approximately 150 °C and could extend as high as 900 °C to complete the degradation process, accompanied by devolatilization with charring (Haz et al. 2019).

The PVA matrix completely decomposed within a temperature range of 263 °C and 440 °C, with DT_p at 380 °C (Figure 2). Meanwhile, the incorporation of 1 wt% of untreated PALF in the PVA matrix, demonstrated by 1UPALF/PVA composite showed a significant improvement in thermal stability as the initial and final decomposition temperatures shifted to a higher temperature, at approximately 279 °C and 470 °C, respectively. Moreover, it is clearly shown in Table 3, that the T_{onset} of 1UPALF/PVA composite increases from 323 °C to 350 °C as compared to the PVA. Besides that,

TABLE 3. TGA data of PVA, PALF, and PALF/PVA composites

Sample	T_{onset} (°C)	$T_{5\%}$ (°C)	$T_{10\%}$ (°C)	$T_{50\%}$ (°C)	DT_p (°C)
PVA	323	319	338	425	381
UPALF	29	88	311	407	68
1UPALF/PVA	350	343	363	444	393
2UPALF/PVA	347	343	359	435	394
3UPALF/PVA	347	343	360	439	393
1TPALF/PVA	352	343	362	434	395

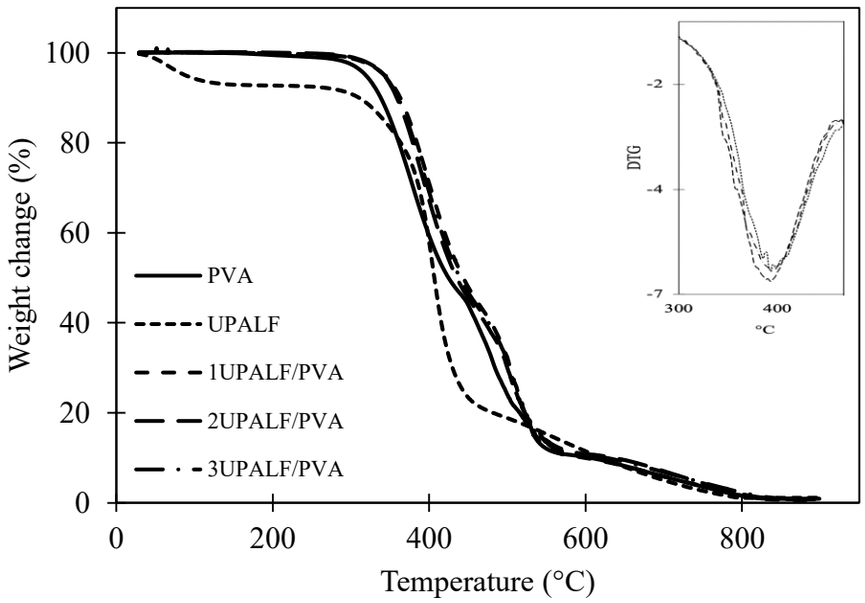

FIGURE 2. Thermograms of TGA and DTG curves (inset figure) of PVA, UPALF, and UPALF/PVA composites at different fibre loadings

the initial thermal decomposition temperatures reflected by the temperatures at 5% and 10% weight loss ($T_{5\%}$ and $T_{10\%}$) are enhanced by the association of PALF into the PVA matrix. The same trend has been observed for $T_{50\%}$, where the thermal stability of the 1UPALF/PVA composite is increased by 19 °C to 444 °C compared to the neat PVA with $T_{50\%}$ at 425 °C. It is suggested that the improvement of thermal stability is due to fiber/matrix interaction during the incorporation of PALF in the PVA matrix. It eventually causes the fibers to absorb heat in the matrix, resist the degradation heat and thus, prolong the degradation process. However, most quantitative values measured, such as T_{onset}, $T_{10\%}$ and $T_{50\%}$ showed a slight reduction as the fiber loading increased. It can be assumed that the high percentage of fiber loading may result in a poor distribution of fibers in the composites. Consequently, this phenomenon will lead to the fiber/fiber interaction which is more vital than the fiber/matrix interaction. The weak interaction between the PVA matrix and PALF is expected to affect the segmental mobility of polymer chains to become unconstraint and thereby decrease the decomposition temperature (Nurazzi et al. 2020).

According to the data presented in Table 3, the T_{onset} of decomposition of 1UPALF/PVA composite is 350 °C. When PALF was treated with alkali treatment, the T_{onset} of 1TPALF/PVA composite slightly increased to 352 °C. As mentioned earlier, it was reported that the lignin might start degrading at a temperature around 150-200 °C, while hemicellulose and cellulosic constituents degrade at higher temperatures (Joseph 2001; Kabir et al. 2011). Therefore, by removing a certain amount of lignin and hemicellulose from the fiber, the thermal stability of the composite is enhanced. It is in agreement with a study observed by Chü (1970) where the improvement in thermal properties occurred as a result of alkali treatment that initiates significant subsidence in hemicellulose and lignin content of the fibers.

DIFFERENTIAL SCANNING CALORIMETRY (DSC)

DSC analysis was governed to determine the composite thermal energy released or absorbed during the heating and cooling process. The DSC measurements were carried out by a heating-cooling-heating cycle. The purpose of the first heating cycle was to remove any thermal history of the composites, which may be influenced by their preparation and storage conditions (Pradeep et al. 2017). Crystallization temperature (T_c), melting temperature (T_m), heat enthalpy of crystallization (ΔH_c), heat enthalpy of melting (ΔH_m), glass-transition temperature (T_g) and

degree of crystallinity (X_c) of PALF/PVA composite films with various fiber loading are presented in Table 4. The T_g is determined in the middle of the inflection point of the glass transition region on the DSC thermogram (Hollaway 2011). The ΔH_m, ΔH_c, and X_c values of the composite films have been normalised according to the actual PVA content in the composites. The degree of crystallisation (X_c) of the composites was calculated according to the Equation (3):

$$Xc(\%) = \frac{\Delta Hm}{\Delta Hm*} \times 100\% \quad (3)$$

where ΔH_m^* is the theoretical heat of fusion of 100% crystallinity of PVA, taken as 138.6 Jg^{-1} (Peppas & Merrill 1976). The DSC thermograms displayed a single peak for the heating and cooling scan of the composites and are shown in Figure 3.

Table 4 presents the DSC results of untreated and treated PALF/PVA composites to study the impact of alkali treatment on the thermal energy response of the composites. The T_m of 1UPALF/PVA composite and 1TPALF/PVA composite remain unchanged at 180 °C. The same observation was recorded for ΔH_m, where only slight changes were observed. The ΔH_m values have a crucial significance where their magnitude is directly proportional to the consequent degree of crystallinity (X_c) of the composite films. As expected, the values of X_c for the composites shared the same trend as ΔH_m values, where the X_c value of 1TPALF/PVA composite was slightly enhanced to 13%, relative to the 1UPALF/PVA composite with X_c value of 12%. Meanwhile for the T_c values, the 1TPALF/PVA composite showed no difference as compared to the 1UPALF/PVA composite.

Glass transition temperature (T_g) is one of the crucial properties when considering composites for a particular end-use. As shown in Table 4, the T_g of 1UPALF/PVA composites was 64 °C. After PALF was treated with alkali treatment, the T_g of 1TPALF/PVA composites was slightly increased to 68 °C. Several studies were also made to investigate the effect of surface modification of fibres by chemical treatment on the thermal properties of the composites. It was reported that treated fibre composites exhibited higher T_g than untreated fibre composites due to the ability of this treatment to remove hemicellulose and lignin from the surface of the fibres. When this happened, the interfacial adhesion between fibres and matrix was improved, thus reducing the mobility of the matrix chains (Negawo et al. 2019). The declined mobility of the matrix chains leads to a higher value of T_g which thereby shows better improvement in the thermal properties of the composites (Fiore, Di Bella & Valenza 2015).

Figure 3 shows the DSC thermogram of neat PVA and TPALF/PVA composites at various fibre loading. The T_m of neat PVA film is 182 °C. Although there appears to be little difference, it was observed that the incorporation of PALF into the composite system shifted the T_m values to a slightly lower temperature. In addition, as the percentage of fibre composition increases in the PALF/PVA

TABLE 4. DSC data of neat PVA and PALF/PVA composites with various fibre loading

Sample	T_g (°C)	T_m (°C)	ΔH_m (Jg^{-1})	X_c (%)	T_c (°C)
PVA	71	182	16	12	131
1UPALF/PVA	64	180	17	12	131
1TPALF/PVA	68	180	18	13	131
2TPALF/PVA	65	179	17	12	132
3TPALF/PVA	64	172	16	11	131

composites, the T_m values also shifted to lower temperatures from 180 °C to 179 °C, and to 172 °C relative to 1, 2 and 3 wt% PALF fibres. From Table 4, incorporating 1 wt% TPALF into the PVA matrix has marginally increased the ΔH_m values to 18 Jg^{-1}, relative to the neat PVA with a ΔH_m value of 16 Jg^{-1}. However, further addition of PALF in the composite system showed no significant changes to the ΔH_m values to 17 Jg^{-1} and 16 Jg^{-1} relative to 2TPALF/PVA and 3TPALF/PVA composites. As expected, the X_c value for the composites followed the same trend as ΔH_m. The X_c value of 1TPALF/PVA composite was slightly enhanced to 13%, relative to the neat PVA of 12%. However, the values showed no significant changes after the addition of 2 and 3 wt% fibre loading. The same observation for T_c values of neat PVA and PALF/PVA composites were studied. It can be seen that the T_c values of TPALF/PVA composites remained unchanged as the fibre loading increases.

CRYSTALLINE PROPERTIES

XRD is a unique method for the determination of the crystallinity of different compounds. Crystallinity index (CI) is a quantitative indicator of crystallinity. The crystallinity plays an important role in determining final properties of composites such as its stiffness and toughness. The calculated CI property of the PALF/PVA composites are tabulated in Table 5.

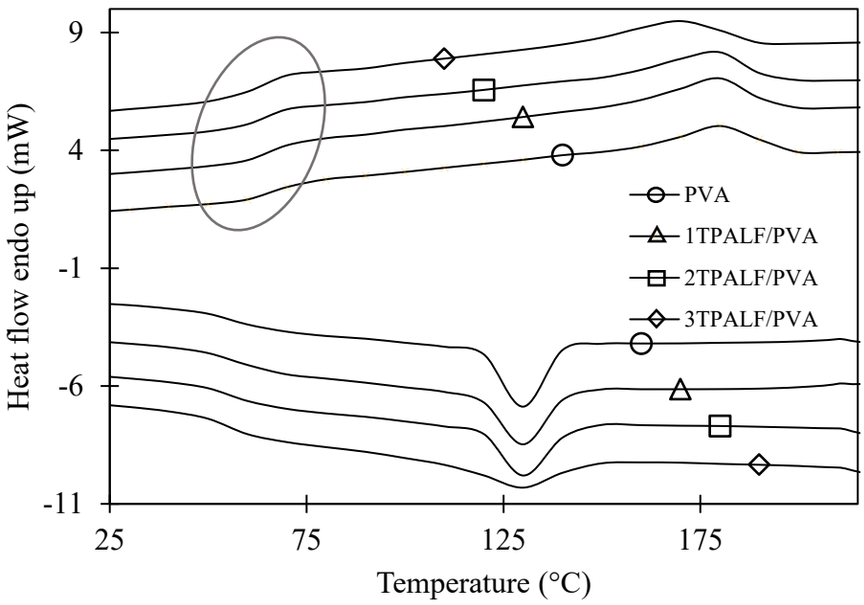

FIGURE 3. DSC thermogram of PVA and TPALF/PVA composites with different fibre loadings

TABLE 5. The crystallinity index data of PALF/PVA composites

Samples	CI (%)
3UPALF/PVA	40
1TPALF/PVA	47
2TPALF/PVA	48
3TPALF/PVA	49

The XRD diffractogram of PALF/PVA composites before and after alkali treatment on the fibre surfaces is shown in Figure 4. It can be observed that the XRD patterns of both 3UPALF/PVA and 3TPALF/PVA composites showed the same diffraction peaks at 2θ from 11° to 32°. According to a previous study, the presence of two diffraction peaks at 2θ, approximately 16° and 22°, which are related to the native cellulose crystalline structure (cellulose I) were attributed to the existence of PALF in the composite (Challabi et al. 2019). As stated earlier, the diffraction patterns of the 3TPALF/PVA composite were found similar to the 3UPALF/PVA composite, indicating that 6% NaOH solution treatment did not change the cellulose's crystal structure. The results obtained were supported by a study that suggested cellulose I allomorph cannot be converted under dilute alkali treatment with NaOH concentration around 5% (Jin et al. 2016). However, in the case of the 3TPALF/PVA composite, the diffraction peak at around 22° becomes sharper than the 3UPALF/PVA composite, confirming the increase in the percentage crystallinity. This is supported by the calculated values of crystallinity, where it can be observed that the crystallinity increased from 40% for 3UPALF/PVA composite to 49% for 3TPALF/PVA composite. In addition, the intensity of the small amorphous hump at 2θ around 11° for the 3TPALF/PVA composite is reduced compared to the 3UPALF/PVA composite. As mentioned earlier, the alkali treatment caused the removal of lignin, hemicellulose, and other amorphous parts at the fibre surface. The presence of NaOH solution during the treatment caused the removal of some amorphous parts in fibres. The amorphous part of fibre which displayed lower molecular weight than cellulose, lack barriers to overcome the NaOH accessibility. Thus, the amorphous part is easier to be hydrolysed during the treatment (Suryanto et al. 2014). These amorphous removals are also expected to increase the crystalline parts of the cellulose (Karimi & Taherzadeh 2016). Along with the diminished amount of amorphous part of fibres, the crystallinity of the PALF fibres is also increased (Prabowo, Pratama & Chalid 2017).

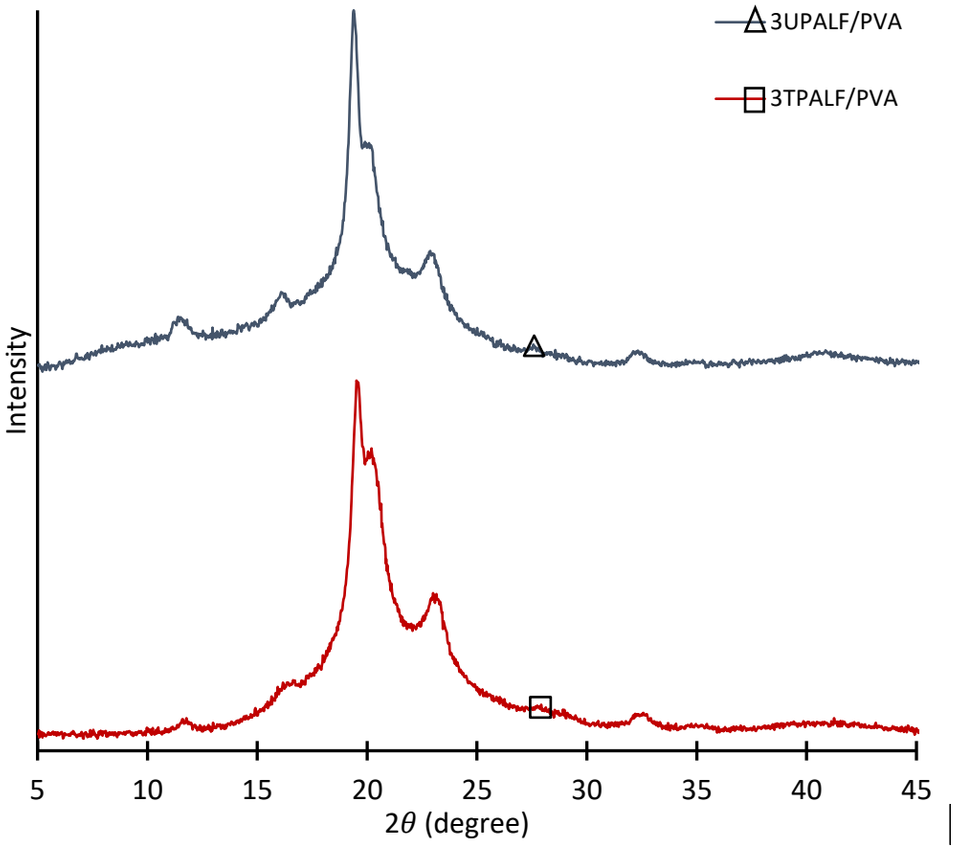

FIGURE 4. The XRD patterns of untreated and treated PALF/PVA composites

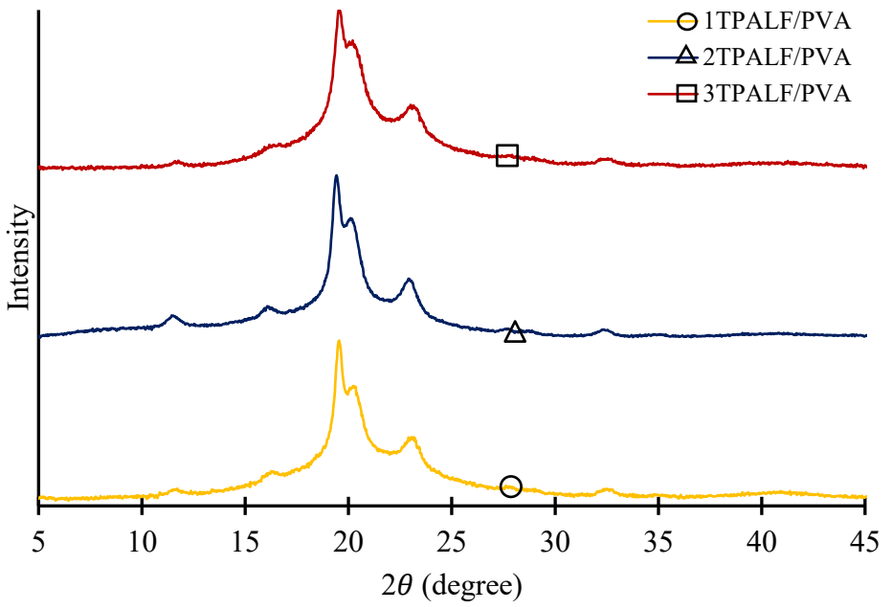

FIGURE 5. The XRD patterns of TPALF/PVA composites at various fibre loading

The TPALF/PVA composites at 1, 2, and 3% fibre loading were characterized by XRD to study the effect of the fibre composition on the matrix PVA crystallinity. As shown in Figure 5, all composites showed the same diffraction patterns from 11° to 32°. In addition, the diffraction peak at 2θ around 20° exhibited a slight variation in intensity, indicating the difference in crystallinity between the composites. The CI of composites is found to be slightly increasing as the fibre loading increases from 47% to 48% then up to 49%, relative to 1, 2, and 3 wt% TPALF/PVA composites. This observation can be explained that TPALF fibres act as nucleating agent which responsible for the crystallization and the partial crystalline growth of PVA matrix to take place. Hence, it may be assumed that the nucleation effect considerably contributed to the increase in crystallinity of composites as the fibre loading increases (Amash & Zugenmaier 2000; Hidalgo-Salazar, Mina & Herrera-Franco 2013; Pickering et al. 2011). In this work, it has been showed that the X_c values derived from the DSC result is in a different range (11-13%) compared to the CI values from the XRD result (40-49%). This difference might have been influenced by other factors and by the facts that these both techniques used different principles to calculate the crystallinity value. The difference in the parameters at which the analysis was conducted also need to be taken into consideration. For instance, XRD analysis assessed the composites at room temperature while DSC analysis analysed at elevated temperature. Thus, it may have contributed to the variance in results.

Tensile Properties

The study of PALF/PVA composite films' mechanical properties is important as it plays a major role in determining a suitable application for various industrial products. Table 6 shows the data measured for tensile strength, tensile strain and tensile modulus of the PALF/PVA composites at various fibre loading.

Tensile Strength and Tensile Modulus

The influence of fibre loading on the tensile properties of PALF/PVA composites is shown in Figure 6. The addition of 1 wt% UPALF into the PVA matrix resulted in an increment in the tensile strength values from 40.1 MPa to 43.6 MPa. Further addition of UPALF up to 3 wt% continuously increased the tensile strength value to 55.4 MPa. It is evident that increasing fibre content in the matrix effectively impacts reinforcement. Similar results have been reported by several authors (Devi, Bhagawan & Thomas 1997; Liu et al. 2005). The bonding and stress transfer effectiveness between the fibre and matrix plays an essential role in governing the tensile strength. When the fibre-reinforced composite is subjected to load, the fibre acts as a carrier of load, and stress is transferred

from the matrix along the fibres, leading to efficacious and uniform stress distribution (Owonubi et al. 2019). At optimum fibre loading, the fibres actively participate in stress transfer activity, thus enhancing the value of the tensile strength of the composites, which explains the good mechanical strength of 3 wt% PALF/PVA composites.

Tensile modulus is a measure of the rigidity of the material. The tensile modulus of PALF/PVA composites with different fibre loading in Figure 6 shows the same behaviour as observed in the tensile strength. The tensile modulus exhibited by pure PVA is 2.0 GPa. The presence of UPALF improved the tensile modulus by 39% to 2.8 GPa with 3 wt% of UPALF loading, relative to the value of tensile modulus of pure PVA. The tensile modulus value increased with the increment in PALF loading, from 2.3 GPa, 2.7 GPa, to 2.8 GPa, relative to 1, 2 and 3 wt% UPALF/PVA composites. The tensile modulus displays the stiffness of the composites. It has been suggested that the improvement in the tensile modulus can be associated with the enhancement in the stiffness and brittleness of the PVA matrix by the addition of PALF. The interfacial adhesion between the fibres and the matrix restrained the movement of polymer chains under loading at lower strain which then permitted the stress transfer from the matrix to the fibres (Ismail & Ishak 2018).

TABLE 6. Tensile properties for PVA and PALF/PVA composites with various fibre loading

Sample	Tensile strength, σ (MPa)	Tensile strain, ε (%)	Tensile modulus, E (GPa)
PVA	40.1	76.1	2.0
1UPALF/PVA	43.6	3.8	2.3
2UPALF/PVA	51.3	3.7	2.7
3UPALF/PVA	55.4	3.5	2.8
3TPALF/PVA	61.6	3.2	2.9

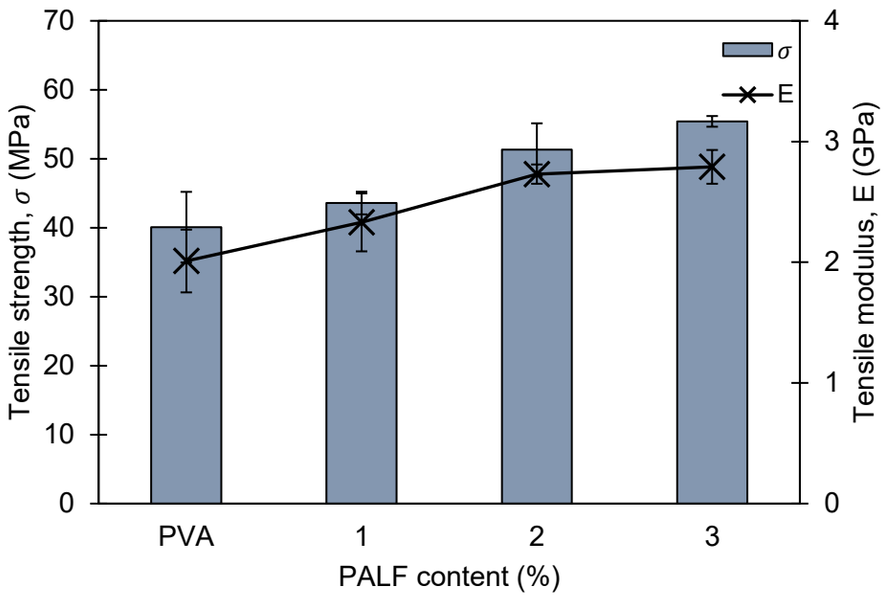

FIGURE 6. Tensile strength and tensile modulus of UPALF/PVA composites at various fibre loadings

The impact of alkali treatment on the tensile properties of the PALF.PVA composites is shown in Figure 7. Upon addition of 3 wt% UPALF, the tensile strength of 3UPALF/PVA composite with its value of 55.4 MPa was measured. Meanwhile, the association of 3 wt% TPALF in the composite resulted in a higher tensile strength value of 61.6 MPa. These can be ascribed to good compatibility between the treated PALF and PVA matrix. The alkali treatment helps remove natural impurities, wax and oil covering the surface of PALF, which reduces the fibre diameter and produces surface roughness (Hamidon et al. 2019). This will further improve fibre/matrix mechanical interlocking and thus, enhance the overall tensile strength of the composites. The 3TPALF/PVA composite exhibit a higher tensile modulus of 2.9 GPa than the 3UPALF/PVA composite with 2.8 GPa recorded. The increment in tensile modulus value could be due to the improvement in the stiffness of fibres due to the surface treatment. This findings are also supported by the XRD results that we obtained earlier. The reduction of amorphous part of the fibre caused by the alkali treatment has increased the crystallinity of the composites, which consequently resulting in higher stiffness properties.

Tensile Strain

Tensile strain refers to material ductility. As shown in Table 6, the addition of UPALF into the composites system has greatly influenced tensile strain values. The tensile strain for the PVA film was 76.1%. The addition of 1 wt% UPALF decreased the tensile strain value to 3.8%. As expected, the tensile strain continued to decrease gradually with an increment in fibre loading from 1 wt% to 3 wt%. The tensile strain reduced from 3.8% for 1 wt% to 3.7% and 3.5% with the addition of UPALF of 2 wt% and 3 wt%, respectively. It could be suggested that the presence of natural fibres hindered the mobility of the polymer chains in the matrix. Therefore, the composites became stiffer as the ratio of elasticity matrix phases was replaced by increasing fibre content (Panyasart et al. 2014).

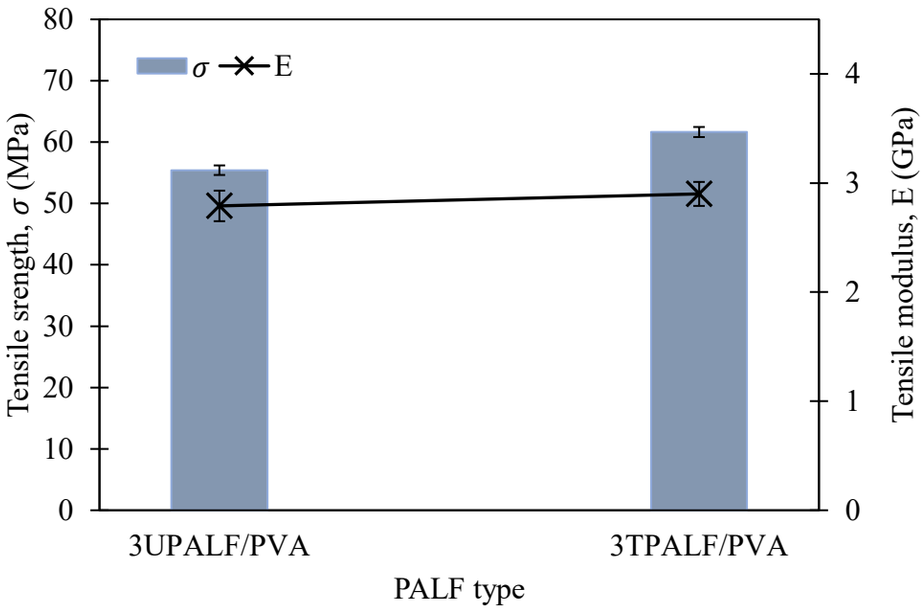

FIGURE 7. Tensile strength and tensile modulus of untreated and treated PALF/PVA composites

Conclusions

This study fabricated neat PVA and PALF reinforced PVA composite films using melt processing method. Alkali treatment was conducted to treat the fibre surfaces, and three compositions of fibre loading (1, 2, 3 wt%) were used in this work. Based on the results, the tensile strength and tensile modulus of the UPALF composites increased linearly with the increment in fibre loading. In addition, mechanical properties including tensile strength and tensile modulus of TPALF reinforced composites were remarkably improved compared to those untreated PALF composites. Meanwhile, tensile strain values decreased gradually with increment in fibre loading from 1 to 3 wt%. The incorporation of PALF as reinforcement in PVA composites has enhanced the thermal stability of the overall composites. Nevertheless, as PALF loading increased, the thermal stability of the composites was slightly reduced due to the poor distribution of fibres in the composites. Fibre surface treatment using 6 % NaOH solution has slightly improved the thermal decomposition of composites compared to the untreated PALF composites. Next, the melting temperature of the composites was found to occur at a slightly lower temperature compared to the neat PVA matrix. However, no significant improvement was found in the composites' melting temperature with treated fibres. The removal of unwanted materials from the fibre surface through alkali treatment has enhanced the crystalline parts of the cellulose. Thus, the crystallinity of the PALF fibres increased which later improved the crystalline properties of the composites. This is believed to result in a new material with the ability to replace commodity plastics.

Acknowledgements

We would like to thank the Ministry of Higher Education, Malaysia for the Fundamental Research Grant Scheme (FRGS/1/2022/STG04/UM/02/7) awarded to Dr. Nor Mas Mira Abd Rahman. The authors also gratefully acknowledge the financial support for part of this project from the Universiti Malaya under the RU Grant Faculty Program (RF025B-2018) and RU Grant SATU (ST043-2021).

References

Akhtar, M.N., Sulong, A.B., Radzi, M.K.F., Ismail, N.F., Raza, M.R., Muhamad, N. & Khan, M.A. 2016. Influence of alkaline treatment and fiber loading on the physical and mechanical properties of kenaf/polypropylene composites for variety of applications. *Progress in Natural Science: Materials International* 26(6): 657-664.

Amash, A. & Zugenmaier, P. 2000. Morphology and properties of isotropic and oriented samples of cellulose fibre–polypropylene composites. *Polymer* 41(4): 1589-1596.

Amiandamhen, S., Meincken, M. & Tyhoda, L. 2020. Natural fibre modification and its influence on fibre-matrix interfacial properties in biocomposite materials. *Fibers and Polymers* 21: 677-689.

Asim, M., Jawaid, M., Abdan, K. & Nasir, M. 2018. Effect of alkali treatments on physical and mechanical strength of pineapple leaf fibres. *IOP Conference Series: Materials Science and Engineering* 290(1): 012030.

Asim, M., Abdan, K., Jawaid, M., Nasir, M., Dashtizadeh, Z., Ishak, M. & Hoque, M.E. 2015. A review on pineapple leaves fibre and its composites. *International Journal of Polymer Science* 6: 1-16.

Challabi, A., Chieng, B.W., Ibrahim, N., Ariffin, H. & Zainuddin, N. 2019. Effect of superheated steam treatment on the mechanical properties and dimensional stability of PALF/PLA biocomposite. *Polymers* 11(3): 482.

Chand, N. & Fahim, M. 2021. 1 - Natural fibers and their composites. In *Tribology of Natural Fiber Polymer Composites.* 2nd ed. Woodhead Publishing.

Chü, N. 1970. The conformation of the anhydrocellobiose units in cellulose I and II. *Journal of Applied Polymer Science* 14(12): 3129-3136.

Devi, L.U., Bhagawan, S.S. & Thomas, S. 1997. Mechanical properties of pineapple leaf fiber-reinforced polyester composites. *Journal of Applied Polymer Science* 64(9): 1739-1748.

Fan, M. & Naughton, A. 2016. Mechanisms of thermal decomposition of natural fibre composites. *Composites Part B: Engineering* 88: 1-10.

Fiore, V., Di Bella, G. & Valenza, A. 2015. The effect of alkaline treatment on mechanical properties of kenaf fibers and their epoxy composites. *Composites Part B: Engineering* 68: 14-21.

Hamidon, M.H., Sultan, M.T.H., Ariffin, A.H. & Shah, A.U.M. 2019. Effects of fibre treatment on mechanical properties of kenaf fibre reinforced composites: A review. *Journal of Materials Research and Technology* 8(3): 3327-3337.

Haz, A., Jablonsky, M., Surina, I., Kačík, F., Bubenikova, T. & Durkovic, J. 2019. Chemical composition and thermal behavior of kraft lignins. *Forests* 10: 483.

Hidalgo-Salazar, M.A., Mina, J.H. & Herrera-Franco, P.J. 2013. The effect of interfacial adhesion on the creep behaviour of LDPE–Al–Fique composite materials. *Composites Part B: Engineering* 55: 345-351.

Hollaway, L.C. 2011. 1 - Key issues in the use of fibre reinforced polymer (FRP) composites in the rehabilitation and retrofitting of concrete structures. In *Service Life Estimation and Extension of Civil Engineering Structures*. Woodhead Publishing.

Islam, M., Pickering, K. & Foreman, N. 2011. Influence of alkali fiber treatment and fiber processing on the mechanical properties of hemp/epoxy composites. *Journal of Applied Polymer Science* 119: 3696-3707.

Ismail, N. & Ishak, Z. 2018. Effect of fiber loading on mechanical and water absorption capacity of polylactic acid/polyhydroxybutyrate-co-hydroxyhexanoate/kenaf composite. *IOP Conference Series: Materials Science and Engineering* 368: 012014.

Jayasekara, R., Harding, I., Bowater, I., Christie, G.B.Y. & Lonergan, G.T. 2004. Preparation, surface modification and characterisation of solution cast starch PVA blended films. *Polymer Testing* 23(1): 17-27.

Jin, E., Guo, J., Yang, F., Zhu, Y., Song, J., Jin, Y. & Rojas, O.J. 2016. On the polymorphic and morphological changes of cellulose nanocrystals (CNC-I) upon mercerization and conversion to CNC-II. *Carbohydrate Polymers* 143: 327-335.

Joseph, S.T., Pillai, C.K.S., Prasad, V.S., Groeninckx, G. & Sarkissova, M. 2003. The thermal and crystallisation studies of short sisal fibre reinforced polypropylene composites. *Composites Part A: Applied Science and Manufacturing* 34: 253-266.

Kabir, M.M., Wang, H., Aravinthan, T., Cardona, F. & Lau, K.T. 2011. Effects of natural fibre surface on composite properties: A review. *Proceedings of the 1st International Postgraduate Conference on Engineering, Designing and Developing the Built Environment for Sustainable Wellbeing (eddBE 2011*). pp. 94-99.

Kalambettu, A., Damodaran, A., Dharmalingam, S. & Vallam. 2015. Evaluation of biodegradation of pineapple leaf fiber reinforced PVA composites. *Journal of Natural Fibers* 12: 39-51.

Karimi, K. & Taherzadeh, M.J. 2016. A critical review of analytical methods in pretreatment of lignocelluloses: Composition, imaging, and crystallinity. *Bioresource Technology* 200: 1008-1018.

Liu, W., Misra, M., Askeland, P., Drzal, L.T. & Mohanty, A.K. 2005. 'Green' composites from soy based plastic and pineapple leaf fiber: Fabrication and properties evaluation. *Polymer* 46(8): 2710-2721.

Lopattananon, N., Panawarangkul, K., Sahakaro, K. & Ellis, B. 2006. Performance of pineapple leaf fiber–natural rubber composites: The effect of fiber surface treatments. *Journal of Applied Polymer Science* 102(2): 1974-1984.

Lu, Y., Lu, Y.C., Hu, H.Q., Xie, F.J., Wei, X.Y. & Fan, X. 2017. Structural characterization of lignin and its degradation products with spectroscopic methods. *Journal of Spectroscopy* 2017: 8951658.

McKeen, L.W. 2017. Introduction to the mechanical, thermal, and permeation properties of plastics and elastomer films. In *Film Properties of Plastics and Elastomers.* 4th ed. William Andrew Publishing.

Mohamed, A.R. 2009. Characterization of pineapple leaf fibers from selected Malaysian cultivars. *Journal of Food, Agriculture & Environment* 7(1): 235-240.

Negawo, T.A., Polat, Y., Buyuknalcaci, F.N., Kilic, A., Saba, N. & Jawaid, M. 2019. Mechanical, morphological, structural and dynamic mechanical properties of alkali treated Ensete stem fibers reinforced unsaturated polyester composites. *Composite Structures* 207: 589-597.

Nopparut, A. & Amornsakchai, T. 2016. Influence of pineapple leaf fiber and it's surface treatment on molecular orientation in, and mechanical properties of, injection molded nylon composites. *Polymer Testing* 52: 141-149.

Nurazzi, N.M., Khalina, A., Sapuan, S.M., Ilyas, R.A., Rafiqah, S.A. & Hanafee, Z.M. 2020. Thermal properties of treated sugar palm yarn/glass fiber reinforced unsaturated polyester hybrid composites. *Journal of Materials Research and Technology* 9(2): 1606-1618.

Owonubi, S., Agwuncha, S., Anusionwu, C., Revaprasadu, N. & Rotimi, S. 2019. Fiber-matrix relationship for composites preparation. In *Composites from Renewable and Sustainable Materials*. Intechopen.

Panyasart, K., Chaiyut, N., Amornsakchai, T. & Santawitee, O. 2014. Effect of surface treatment on the properties of pineapple leaf fibers reinforced polyamide 6 composites. *Energy Procedia* 56: 406-413.

Peng, Z. & Kong, L. 2007. A thermal degradation mechanism of polyvinyl alcohol/silica nanocomposites. *Polymer Degradation and Stability* 92: 1061-1071.

Peppas, N.A. & Merrill, E.W. 1976. Differential scanning calorimetry of crystallized PVA hydrogels. *Journal of Applied Polymer Science* 20(6): 1457-1465.

Peresin, M.S., Habibi, Y., Zoppe, J.O., Pawlak, J.J. & Rojas, O.J. 2010. Nanofiber composites of polyvinyl alcohol and cellulose nanocrystals: Manufacture and characterization. *Biomacromolecules* 11(3): 674-681.

Pickering, K.L., Sawpan, M.A., Jayaraman, J. & Fernyhough, A. 2011. Influence of loading rate, alkali fibre treatment and crystallinity on fracture toughness of random short hemp fibre reinforced polylactide bio-composites. *Composites Part A: Applied Science and Manufacturing* 42(9): 1148-1156.

Prabowo, I., Pratama, J. & Chalid, M. 2017. The effect of modified ijuk fibers to crystallinity of polypropylene composite. *IOP Conference Series: Materials Science and Engineering* 223: 012020.

Pradeep, S.A., Kharbas, H., Turng, L.S., Avalos, A., Lawrence, J.G. & Pilla, S. 2017. Investigation of thermal and thermomechanical properties of biodegradable PLA/PBSA composites processed via supercritical fluid-assisted foam injection molding. *Polymers* 9(1): 22.

Sarah, Y., Rahman, W.A.W.A., Majid, R.A., Yahya, W.J., Adrus, N., Hasannuddin, A.K. & Low, J.H. 2018. Optimization of pineapple leaf fibre extraction methods and their biodegradabilities for soil cover application. *Journal of Polymers and the Environment* 26: 319-329.

Suryanto, H., Marsyahyo, E., Irawan, Y. & Soenoko, R. 2014. Effect of alkali treatment on crystalline structure of cellulose fiber from mendong (*Fimbristylis globulosa*) straw. *Key Engineering Materials* 595: 720-724.

WWF Malaysia. 2020. *Releases Report Proposing Effective Solution to Mitigate Plastic Pollution in Malaysia*. Accessed November 8, 2021. https://www.wwf.org.my/?28105/WWF-Releases-Report-Proposing-Effective-Solution-to-Mitigate-Plastic-Pollution-in-Malaysia

Zin, M.H., Abdan, K., Mazlan, N., Zainudin, E.S. & Liew, K.E. 2018. The effects of alkali treatment on the mechanical and chemical properties of pineapple leaf fibres (PALF) and adhesion to epoxy resin. *IOP Conference Series: Materials Science and Engineering* 368(1): 012035.

*Corresponding author; email: nmmira@um.edu.my